Supporting information for manuscript Molecular dynamics simulations and solid-state nuclear magnetic resonance spectroscopy measurements of C-H bond order parameters and effective correlation times in a POPC-GM3 bilayer

Simon Fridolf[1], Mona Koder Hamid[2], Leo Svenningsson[1], Marie Skepö[2], Emma Sparr[1], Daniel Topgaard[1]

[1]Division of Physical Chemistry, Lund University, Lund, Sweden; [2]Division of Theoretical Chemistry, Lund University, Lund, Sweden.

October 2022

Molecular dynamics simulations

All-atom molecular dynamics (MD) simulations were done for POPC bilayers with and without 30 mol% GM3 using the GROMACS package (version 2021)[1] and modelled with the CHARMM36 force field[2] and CHARMM modified TIP3P water model.[3,4] The initial bilayers were constructed with the CHARMM-GUI Membrane Builder.[5] The POPC bilayer had 80 lipids in each leaflet and was hydrated with 13125 water molecules. The second bilayer had 56 POPC and 24 GM3 lipids in each leaflet and was hydrated with 10940 water molecules and neutralized with 48 potassium ions. A rectangular box was used with the initial dimensions 7.4 x 7.4 x 11.9 nm and 7.3 x 7.3 x 11.9 nm for the POPC and POPC-GM3 bilayers, respectively. Periodic boundary conditions were applied in all directions. Initial structures were minimized with the steepest descent algorithm. Equilibration with position restraints on the lipids was done in six steps following the standard CHARMM-GUI protocol for a total of 2250 ps. Further equilibration was done with position restraints lifted and used the Verlet leap-frog integrator with a 2 fs time step and frames saved every 100 ps, for 64 ns and 100 ns, for POPC and POPC with 30 mol% GM3 respectively. Production runs were then done, also with the Verlet leap-frog integrator using a 2 fs time step and frames saved every 100ps for a total of 1 μs, with separate groups for the lower and upper leaflet for center of mass motion removal to ensure no drifting of the leaflets. Pair lists were generated with a Verlet cutoff-scheme for the non-bonded interactions. Van der Waals interactions were calculated with a force-switch and cut off radius of 1.2 nm. Long-ranged electrostatics were managed with Particle-Mesh Ewald[6] using a grid spacing of 0.12 nm and cut-off radius of 1.2 nm. Bonds with hydrogen were constrained with the LINCS algorithm.[7] Rigid water was used together with the SETTLE algorithm.[8] Temperature was set at 303.15 K using the Nose-Hoover thermostat[9,10] with a coupling constant of 1.0 ps. Pressure was maintained at 1.0 bar with a Parrinello-Rahman barostat[11] using semi-isotropic pressure coupling, separating the lateral and normal dimensions relative to the bilayer, with a coupling constant of 5.0 ps and a compressibility of 4.5×10^{-5} bar^{-1}.

All analysis were done on the complete production runs of 1 μs. Order parameters S_{CH} were calculated with code from the NMRlipids project.[12] S_{CH} is defined according to Eq. 2 in the main text and can be calculated from the trajectories as follows:

$$S_{CH} = \frac{1}{2NM} \sum_{m=1}^{M} \sum_{n=1}^{N} \left(\frac{3 r_{nm,z}^2}{|\vec{r}_{nm}|^2} - 1 \right), \tag{S1}$$

where $\vec{r}_{nm}$ is the vector for the C-H bond of molecule m at time frame n, relative to a coordinate axis placing the z-axis parallel to the bilayer normal. The sum goes through all M lipids, and all N frames of the analyzed trajectory.

The simulations were extended further for a minimum of 1 ns, in steps where frames for the trajectory were saved more frequently, down to the limit of 2 fs. The reorientational autocorrelation for the fast regime, $g_f(\tau)$, was calculated using the "rotacf" function in Gromacs. The length of simulations determines the maximum time τ, and the shortest time between frames, 2 fs, the minimum τ probed. At the ms range $g_f(\tau)$ is approximated as S_{CH}^2.

Electron densities were calculated using the gromacs command "gmx density" and assigning atoms the number of electrons according to their atomic number. From the electron density of the lipid bilayer, the head-to-head distance D_{HH} is obtained from the distance between the maximum peaks,[13,14] see figures S1 and S2. Number densities were calculated with "gmx density" and converted to volume probabilities following the method by Petrache et al.[15] with the number density for each lipid element multiplied by a correction factor, see table S1. The bilayer thickness, D_B and hydrophobic thickness, D_C are found from Gibbs dividing surface of the volume probability of water and the hydrocarbon chains respectively[16], see figures S3 and S4.

Table S1: The volumetric correction parameters used to convert the number densities to volume probabilities.

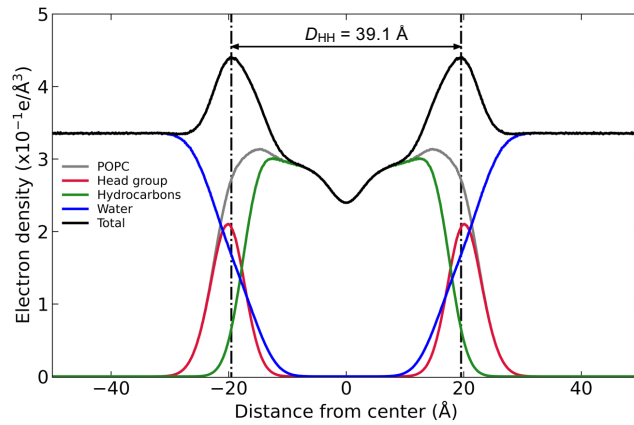| Group	Volumetric correction factor	
	POPC ($Å^3$)	POPC:GM3 7:3 ($Å^3$)
POPC – PCN	6.00	6.00
POPC – Choline CH_3	8.00	7.40
POPC – γ	9.70	9.10
POPC – CH	3.50	8.75
POPC – CH_2	9.80	8.75
POPC – CH_3	11.80	11.10
GM3 – NeuAc	---	6.80
GM3 – Glucose	---	9.20
GM3 – Galactose	---	7.50
GM3 – CH_2, CHNH, CHOH, CO	---	8.75
GM3 – CH_3	---	11.10
Water	9.94	9.945

Figure S1: Electron density across the POPC bilayer (grey) and its headgroup (red) and hydrocarbon tails (green), as well as that of water (blue) and the total density (water+lipids). The head-to-head distance D_{HH} is illustrated with the double arrow in the figure.
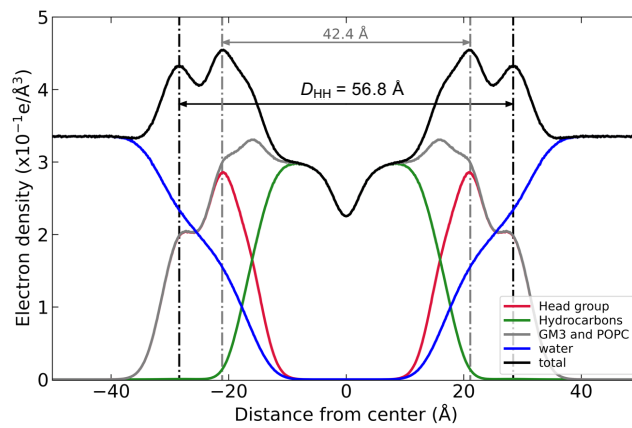
Figure S2. Electron density across the GM3:POPC 3:7 bilayer (gray) and its head group (red) and hydrocarbon tails (green), where that of GM3 and POPC have been grouped together, as well as that of water (blue) and the total density (water+lipids). The head-to-head distances D_{HH} corresponding to the two maxima in the total density are illustrated with the double arrows in the figure.

Figure S3. The volume probability across the z-axis for the POPC lipid tails including CH and CH_2, (green), methyl groups (orange) and its head group (red), as well as water (blue). Vertical lines showing Gibbs dividing surface for water (dashed dotted) and hydrocarbons (dotted) from which the bilayer thickness D_B, and hydrophobic

thickness, D_C (illustrated with double arrows) are determined. Top graph shows the sum of all components, ideally equal to one.
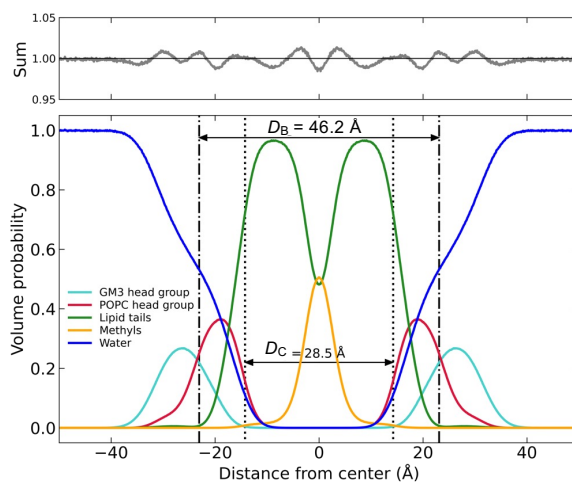
Figure S4. The volume probability across the z-axis for the GM3 and POPC lipid tails, including CH, CH$_2$, CHNH, CHOH, CO groups (green), methyl groups (orange), the head groups of POPC (red) and GM3 (cyan), as well as water (blue). Vertical lines showing Gibbs dividing surface for water (dashed dotted) and hydrocarbons (dotted) from which the bilayer thickness D_B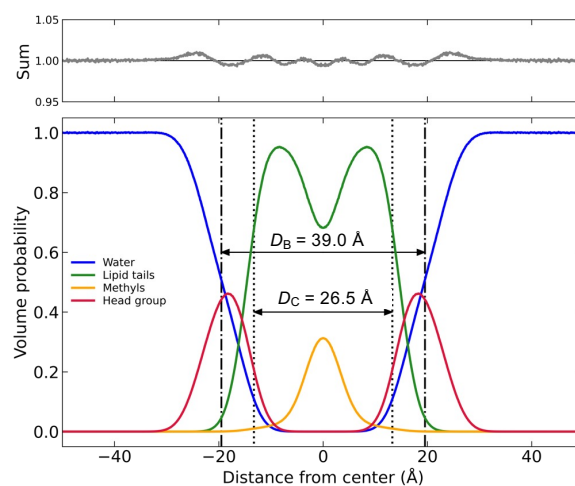, and hydrophobic thickness, D_C (illustrated with double arrows) are determined. Top graph shows the sum of all components, ideally equal to one.
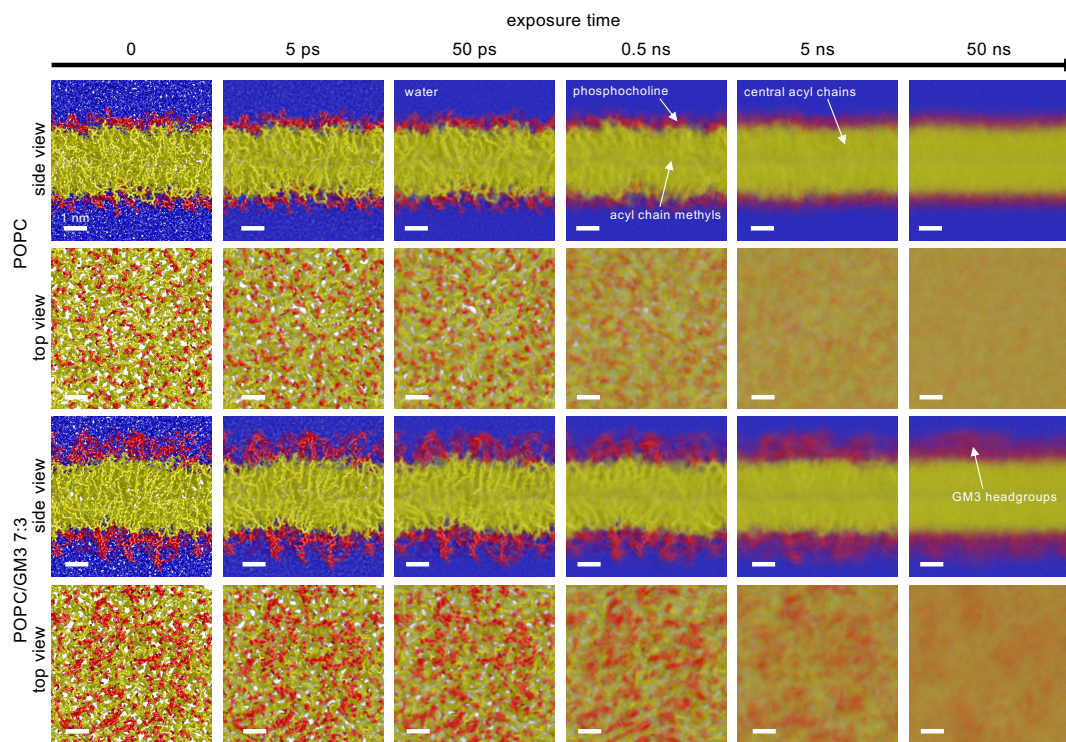
Figure S5 MD simulation snapshots of POPC and POPC with 30 mol% GM3 at varying expoure times (motion blur), illustrating the timescale of segmental motions. The colors identify different molecular segments: blue (water), red (headgroups) and yellow (hydrophobic tails). White labels and arrows annotate the sharp-to-blur transition for water, the POPC headgroup, the central acyl chain carbons, the terminal methyl groups on the acyl chains and the GM3 headgroup, which roughly corresponds to the effective correlation time τ_e for rotational diiffusion of molecular segments. The view scale for all snapshots is the same and the length of the white scale

bar represents 1 nm. The field of view is 1.1 times the box sizes in the x and y directions and 0.7 in the z-direction. Periodic boundary conditions were applied in all directions.

NMR spectroscopy
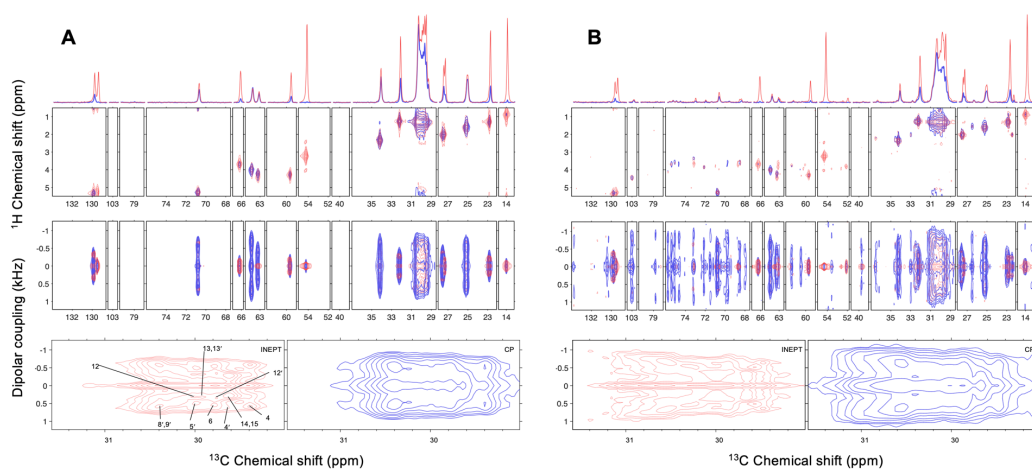
Figure S6: 1D, HETCOR[17] and R-PDLF[18] MAS NMR spectra of an equilibrium phase of POPC in the absence (A) and presence (B) of 30 mol% GM3, recorded at 303 K with 5 kHz MAS and 68 kHz SPINAL64 ^{1}H-decoupling during ^{13}C acquisition. All experiments were done using both INEPT (red) and CP (blue) for ^{1}H-^{13}C polarisation transfer. The bottom panels are zoom-ins of the hydrophobic tails CH_2 signal from the R-PDLF spectra with POPC peak assignments from Ferreira et al.[19].
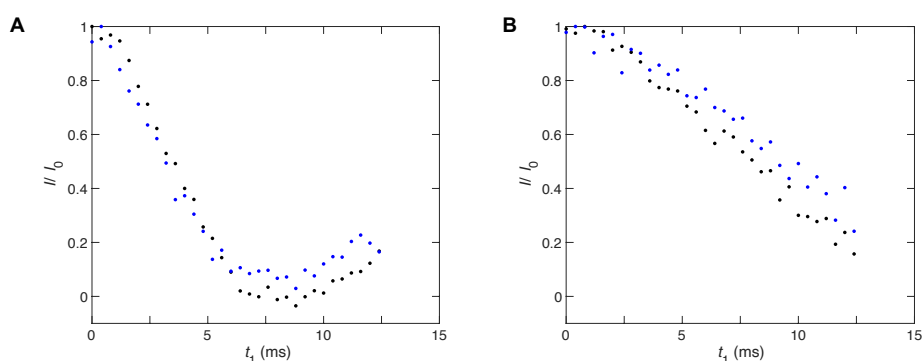
Figure S7: ^{1}H-^{13}C Dipolar modulation of the normalised intensity with time in the indirect dimension t_1 for the ^{13}C tail terminal methyl signals R18, R16', 18 and 16' (A) and choline γ-methyls (B) during the R-PDLF experiment for samples of POPC in the absence (black) and presence (blue) of 30 mol% GM3, recorded at 303 K with INEPT for polarization transfer, 5 kHz MAS and 68 kHz SPINAL64 ^{1}H-decoupling during ^{13}C acquisition. Small values of the order parameter $|S_{CH}|$ can be estimated from the minimum in the time-domain signal, where $\Delta v^{R-PDLF} = 2/t_{min}$,[20] from which both values of $|S_{CH}|$ was estimated to approximately 0.004 for the tail terminal methyls. Note that $|S_{CH}|$ values in the main text were obtained from time-domain fits to Eq. 9 rather than simple inspection of the minimum. The indirect dimension was sampled in 32 steps with 400 μs linear increments.
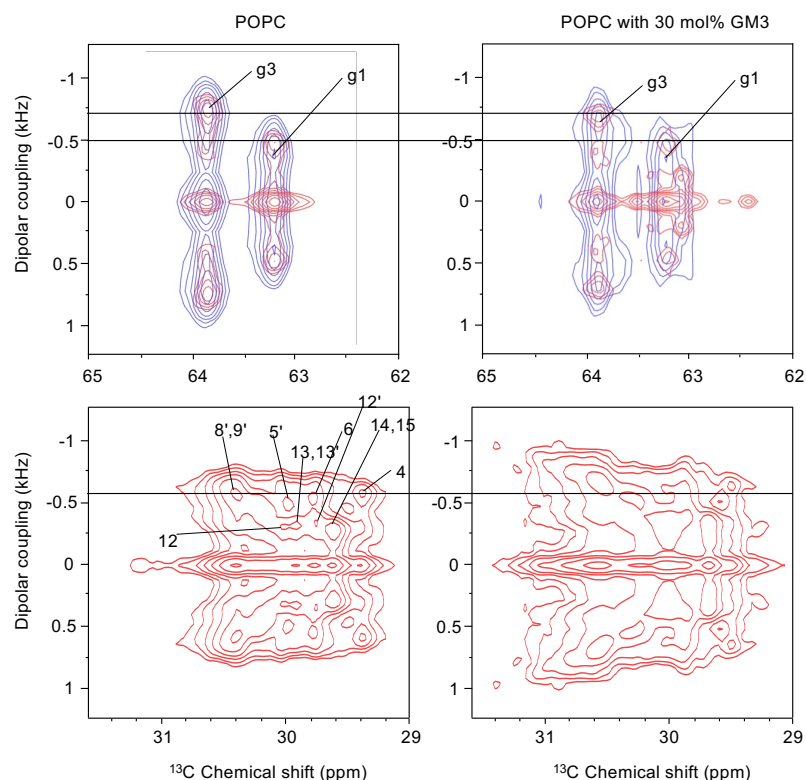
Figure S8: R-PDLF[18] MAS NMR spectra of an equilibrium phase of POPC in the absence (left column) and presence (right column) of 30 mol% GM3, recorded at 303 K with 5 kHz MAS and 68 kHz SPINAL64 [1]H-decoupling during ^{13}C acquisition. Peak labels are from Fig. 1 in the main text, where g3 and g2 refers to glycerol carbons in POPC. Experiments were done using INEPT (red) and CP (blue) for [1]H-^{13}C polarisation transfer. The horizontal black lines are guides for the eye used to illustrating splittings that are affected by the presence of GM3.

Table S2: NMR-derived order parameters $|S_{CH}|$, effective correlation times τ_e and $R_{1\rho}$ and R_1 relaxation rate constants for POPC with 30 mol% GM3 at 303 K.

Carbon label	δ^{13}C (ppm)	δ^1H (ppm)	$|S_{CH}|$ (manual)	$|S_{CH}|$ (fit)	$R_{1\rho}$ (s^{-1})	R_1 (s^{-1})	τ_e (s)
R18,R16',18,16'	14.00	0.89	0.00	0.02	2.06	0.34	1.65·10^{-10}
III11	22.46	2.01	0.07	-	-	-	-
R17,R15',17,15'	22.84	1.30	0.06	0.07	3.65	0.57	4.43·10^{-10}
3,3'	25.17	1.60	0.19	0.19	12.60	2.20	1.55·10^{-9}
R3,R6	26.48	1.58	0.26	0.27	11.51	3.45	1.57·10^{-9}
R3'	27.40	1.56	0.12	-	-	-	-
8	27.40	2.03	0.13	-	-	-	-
11	27.55	2.03	0.06	-	-	-	-
R4'	29.12	1.32	0.21	-	-	-	-
4	29.47	1.32	0.19	-	-	-	-
R5'	29.49	1.32	0.21	-	-	-	-
14,15	29.65	1.32	0.11	-	-	-	-
12,12'	29.84	1.32	0.12	-	-	-	-
4'	29.84	1.32	0.19	-	-	-	-
6	29.84	1.32	0.18	-	-	-	-
R13	29.85	1.32	0.11	-	-	-	-
R12'	29.86	1.32	0.12	-	-	-	-
13,13'	29.96	1.32	0.11	-	-	-	-

5	29.96	1.32	0.19	-	-	-	-
R13'	30.00	1.32	0.09	-	-	-	-
R1**4**	30.02	1.32	0.11	-	-	-	-
R15	30.02	1.32	0.10	-	-	-	-
5'	30.09	1.32	0.19	-	-	-	-
12	30.09	1.32	0.11	-	-	-	-
10'	30.19	1.32	0.16	-	-	-	-
11'	30.19	1.32	0.15	-	-	-	-
R10',R11,R12	30.20	1.32	0.16	-	-	-	-
R11'	30.20	1.32	0.15	-	-	-	-
7	30.35	1.32	0.16	-	-	-	-
6'	30.50	1.32	0.20	0.22	14.38	1.42	$1.92 \cdot 10^{-9}$
7'	30.58	1.32	0.20	0.22	14.38	1.42	$1.92 \cdot 10^{-9}$
8'	30.67	1.32	0.19	0.22	14.38	1.42	$1.92 \cdot 10^{-9}$
9'	30.76	1.32	0.19	0.22	14.38	1.42	$1.92 \cdot 10^{-9}$
R9,R10	30.78	1.32	0.22	0.22	14.38	1.42	$1.92 \cdot 10^{-9}$
R8',R9'	30.78	1.32	0.20	0.22	14.38	1.42	$1.92 \cdot 10^{-9}$
R7,R8	30.98	1.32	0.24	0.22	14.38	1.42	$1.92 \cdot 10^{-9}$
R6',R7'	30.98	1.32	0.20	0.22	14.38	1.42	$1.92 \cdot 10^{-9}$
R14',R16	32.22	1.28	0.08	0.10	4.98	0.79	$6.06 \cdot 10^{-10}$
16,14'	32.23	1.26	0.09	0.10	4.98	0.79	$6.06 \cdot 10^{-10}$
2'	34.24	2.33	0.20	0.14	21.52	2.46	$2.72 \cdot 10^{-9}$
2	34.24	2.33	0.08	0.14	21.52	2.46	$2.72 \cdot 10^{-9}$
R2'	36.50	2.24	0.05	0.19	52.36	2.13	$7.21 \cdot 10^{-9}$
III3	39.73	2.94	0.01	0.19	29.02	2.41	$3.83 \cdot 10^{-9}$
III3	39.73	2.67	0.01	0.01	29.02	2.41	$3.83 \cdot 10^{-9}$
III5	52.09	3.58	0.04	0.04	13.45	2.52	$3.16 \cdot 10^{-9}$
R2	53.57	3.94	0.25	0.29	28.28	1.29	$8.18 \cdot 10^{-9}$
γ	54.31	3.23	0.00	0.01	3.00	2.41	$1.06 \cdot 10^{-10}$
α	59.67	4.29	0.04	0.04	7.69	2.82	$7.59 \cdot 10^{-10}$
I6	61.39	3.77	0.14	0.17	28.9	4.34	$3.53 \cdot 10^{-9}$
I6	61.39	3.77	0.01	0.04	28.9	4.34	$3.54 \cdot 10^{-9}$
II6	63.09	3.63	0.16	0.17	19.3	5.00	$2.17 \cdot 10^{-9}$
II6	63.09	3.85	0.06	0.07	19.3	5.00	$2.17 \cdot 10^{-9}$
g1	63.21	4.23	0.14	0.14	25.30	4.32	$3.06 \cdot 10^{-9}$
g1	63.21	4.43	0.08	0.01	22.30	4.32	$3.06 \cdot 10^{-9}$
III9	63.51	3.80	0.06	-	-	-	-
III9	63.51	4.38	0.06	-	-	-	-
g3	63.86	4.00	0.12	0.15	26.74	4.39	$3.34 \cdot 10^{-9}$
g3	63.86	4.00	0.21	0.21	26.74	4.39	$3.34 \cdot 10^{-9}$
β	66.24	3.67	0.04	0.04	4.99	2.78	$3.93 \cdot 10^{-10}$
II4	68.49	3.57	0.18	0.20	37.17	2.91	$9.98 \cdot 10^{-9}$
III4	68.53	3.93	0.02	0.01	20.16	2.77	$4.94 \cdot 10^{-9}$
III7	68.68	3.82	0.02	0.00	8.14	2.17	$1.78 \cdot 10^{-9}$
II2	69.72	3.54	0.25	0.30	14.30	3.09	$3.59 \cdot 10^{-9}$
R1	69.82	3.81	0.19	0.23	76.51	3.37	$1.06 \cdot 10^{-8}$
R1	69.82	4.20	0.11	0.12	76.51	3.37	$1.06 \cdot 10^{-8}$

g2	70.76	5.27	0.19	0.19	13.06	2.59	$3.15 \cdot 10^{-9}$
III8	72.11	3.84	0.12	0.22	37.03	2.68	$1.01 \cdot 10^{-8}$
III6	73.12	3.63	0.04	0.02	15.50	2.66	$3.69 \cdot 10^{-9}$
I2	73.17	3.33	0.27	0.30	49.60	2.52	$1.43 \cdot 10^{-8}$
I3	74.65	3.57	0.27	0.28	28.21	2.94	$7.71 \cdot 10^{-9}$
I5	75.04	3.66	0.27	0.29	21.33	1.64	$6.00 \cdot 10^{-9}$
II5	75.36	3.67	0.20	0.20	21.96	2.12	$5.81 \cdot 10^{-9}$
II3	75.73	4.07	0.25	0.26	25.29	1.61	$7.08 \cdot 10^{-9}$
I4	78.76	3.71	0.28	0.29	32.21	2.38	$9.07 \cdot 10^{-9}$
I1	102.96	4.44	0.26	0.27	22.26	3.02	$5.89 \cdot 10^{-9}$
II1	103.07	4.44	0.25	0.25	30.87	2.29	$8.49 \cdot 10^{-9}$
10	129.51	5.30	0.03	0.03	3.05	1.78	$4.61 \cdot 10^{-10}$
9	129.77	5.32	0.11	0.11	3.98	1.47	$7.94 \cdot 10^{-10}$
R4	130.52	5.34	0.14	0.23	20.27	1.33	$5.56 \cdot 10^{-9}$
R5	133.76	5.34	0.21	0.27	24.89	2.37	$6.81 \cdot 10^{-9}$

Table S3: MD-derived order parameters S_{CH}, effective correlation times τ_e and $R_{1\rho}$ and R_1 relaxation rate constants calculated with Eq. S1, 4, 6 and 7 respectively for POPC with 30 mol% GM3 at 303 K. The relaxation value for each carbon used to calculate τ_e is the sum of the contributions from all individual bonded protons.

Carbon label	C-H pair	S_{CH}	$R_{1\rho}$ (s⁻¹)	R_1 (s⁻¹)	Sum $R_{1\rho}$ (s⁻¹)	Sum R_1 (s⁻¹)	τ_e (s)
R18	C18S-H18S	-0.06	0.52	0.10	1.96	0.30	$1.60 \cdot 10^{-10}$
R18	C18S-H18T	-0.06	0.77	0.10	-	-	-
R18	C18S-H18U	-0.06	0.68	0.10	-	-	-
R16'	C16F-H16F	-0.04	0.16	0.10	0.48	0.31	$2.19 \cdot 10^{-11}$
R16'	C16F-H16G	-0.04	0.17	0.10	-	-	-
R16'	C16F-H16H	-0.04	0.16	0.10	-	-	-
16'	C316-H16X	-0.04	0.14	0.10	0.52	0.28	$2.73 \cdot 10^{-11}$
16'	C316-H16Y	-0.04	0.18	0.09	-	-	-
16'	C316-H16Z	-0.04	0.21	0.10	-	-	-
18	C218-H18R	-0.04	0.11	0.10	0.35	0.29	$1.11 \cdot 10^{-11}$
18	C218-H18S	-0.04	0.12	0.10	-	-	-
18	C218-H18T	-0.04	0.12	0.10	-	-	-
III11	CT-HT1	-0.02	33.63	0.12	100.47	0.35	$9.29 \cdot 10^{-9}$
III11	CT-HT2	-0.02	33.75	0.12	-	-	-
III11	CT-HT3	-0.02	33.09	0.12	-	-	-
R17	C17S-H17S	-0.15	0.68	0.23	1.50	0.46	$1.62 \cdot 10^{-10}$
R17	C17S-H17T	-0.15	0.82	0.23	-	-	-
R15'	C15F-H15F	-0.15	0.88	0.23	1.55	0.45	$1.70 \cdot 10^{-10}$
R15'	C15F-H15G	-0.15	0.67	0.23	-	-	-
15'	C315-H15X	-0.11	0.54	0.22	1.03	0.44	$9.68 \cdot 10^{-11}$
15'	C315-H15Y	-0.11	0.48	0.22	-	-	-
17	C217-H17R	-0.11	0.45	0.24	0.92	0.47	$7.79 \cdot 10^{-11}$
17	C217-H17S	-0.11	0.47	0.23	-	-	-
3'	C33-H3X	-0.22	5.08	0.97	10.58	1.96	$1.31 \cdot 10^{-9}$
3'	C33-H3Y	-0.20	5.51	0.98	-	-	-
3	C23-H3R	-0.23	7.70	1.38	12.75	2.85	$1.56 \cdot 10^{-9}$
3	C23-H3S	-0.24	5.05	1.47	-	-	-
R3	C3S-H3S	-0.37	122.73	0.67	122.73	0.67	$3.88 \cdot 10^{-8}$

R6	C6S-H6S	-0.31	22.63	1.17	48.26	2.32	$7.06 \cdot 10^{-9}$
R6	C6S-H6T	-0.30	25.63	1.16			
R3'	C3F-H3F	-0.23	45.85	1.51	80.37	3.20	$1.13 \cdot 10^{-8}$
R3'	C3F-H3G	-0.14	34.53	1.69			
8	C28-H8R	-0.12	1.96	1.04	3.97	2.09	$3.36 \cdot 10^{-10}$
8	C28-H8S	-0.12	2.01	1.05	-	-	-
11	C211-H11R	-0.10	1.38	0.83	2.82	1.66	$2.19 \cdot 10^{-10}$
11	C211-H11S	-0.10	1.43	0.83	-	-	-
R4'	C4F-H4F	-0.26	11.54	1.38	18.94	2.82	$2.48 \cdot 10^{-9}$
R4'	C4F-H4G	-0.24	7.40	1.43	-	-	-
4	C24-H4R	-0.23	4.28	1.08	7.82	2.19	$9.03 \cdot 10^{-10}$
4	C24-H4S	-0.23	3.54	1.11	-	-	-
R5'	C5F-H5F	-0.27	9.22	1.01	14.31	2.03	$1.90 \cdot 10^{-9}$
R5'	C5F-H5G	-0.26	5.10	1.02	-	-	-
14	C214-H14R	-0.18	1.30	0.51	2.45	1.03	$2.41 \cdot 10^{-10}$
14	C214-H14S	-0.18	1.15	0.51	-	-	-
15	C215-H15R	-0.16	0.99	0.43	1.95	0.86	$1.86 \cdot 10^{-10}$
15	C215-H15S	-0.16	0.96	0.43	-	-	-
12'	C312-H12X	-0.20	1.54	0.47	3.06	0.93	$3.43 \cdot 10^{-10}$
12'	C312-H12Y	-0.20	1.52	0.47	-	-	-
4'	C34-H4X	-0.24	2.98	0.87	6.40	1.73	$7.46 \cdot 10^{-10}$
4'	C34-H4Y	-0.24	3.41	0.86	-	-	-
6	C26-H6R	-0.22	2.73	0.88	5.44	1.76	$5.98 \cdot 10^{-10}$
6	C26-H6S	-0.22	2.71	0.88	-	-	-
R13	C13S-H13S	-0.26	1.56	0.56	3.38	1.13	$3.75 \cdot 10^{-10}$
R13	C13S-H13T	-0.25	1.82	0.56	-	-	-
R12'	C12F-H12F	-0.23	1.70	0.48	3.19	0.96	$3.59 \cdot 10^{-10}$
R12'	C12F-H12G	-0.23	1.49	0.48	-	-	-
13'	C313-H13X	-0.18	1.12	0.40	2.29	0.80	$2.41 \cdot 10^{-10}$
13'	C313-H13Y	-0.18	1.17	0.40	-	-	-
13	C213-H13R	-0.17	1.27	0.59	2.65	1.17	$2.52 \cdot 10^{-10}$
13	C213-H13S	-0.17	1.38	0.59	-	-	-
5	C25-H5R	-0.25	3.59	0.93	6.80	1.87	$7.94 \cdot 10^{-10}$
5	C25-H5S	-0.25	3.21	0.94	-	-	-
R13'	C13F-H13F	-0.22	1.46	0.40	2.66	0.81	$2.97 \cdot 10^{-10}$
R13'	C13F-H13G	-0.22	1.20	0.40	-	-	-
R14	C14S-H14S	-0.25	1.43	0.49	3.32	0.98	$3.82E \cdot 10^{-10}$
R14	C14S-H14T	-0.25	1.89	0.49	-	-	-
R15	C15S-H15S	-0.22	1.19	0.42	2.45	0.84	$2.63 \cdot 10^{-10}$
R15	C15S-H15T	-0.22	1.26	0.42	-	-	-
5'	C35-H5X	-0.25	2.89	0.75	6.05	1.51	$7.23 \cdot 10^{-10}$
5'	C35-H5Y	-0.25	3.16	0.76	-	-	-
12	C212-H12R	-0.16	1.47	0.68	2.87	1.36	$2.63 \cdot 10^{-10}$
12	C212-H12S	-0.16	1.41	0.68	-	-	-
10'	C310-H10X	-0.24	1.88	0.55	3.88	1.10	$4.51 \cdot 10^{-10}$
10'	C310-H10Y	-0.24	2.00	0.55	-	-	-
11'	C311-H11X	-0.22	1.60	0.51	3.27	1.03	$3.65 \cdot 10^{-10}$

11'	C311-H11Y	-0.22	1.67	0.52	-	-	-
R11	C11S-H11S	-0.28	2.19	0.70	4.84	1.39	$5.71 \cdot 10^{-10}$
R11	C11S-H11T	-0.27	2.65	0.70	-	-	-
R12	C12S-H12S	-0.28	2.13	0.62	5.04	1.24	$6.17 \cdot 10^{-10}$
R12	C12S-H12T	-0.27	2.91	0.62	-	-	-
R10'	C10F-H10F	-0.26	2.81	0.59	5.01	1.18	$6.14 \cdot 10^{-10}$
R10'	C10F-H10G	-0.26	2.20	0.59	-	-	-
R11'	C11F-H11F	-0.25	2.21	0.53	3.95	1.06	$4.66 \cdot 10^{-10}$
R11'	C11F-H11G	-0.25	1.74	0.53	-	-	-
7	C27-H7R	-0.21	2.49	0.86	4.94	1.73	$5.25 \cdot 10^{-10}$
7	C27-H7S	-0.21	2.45	0.87	-	-	-
6'	C36-H6X	-0.26	2.43	0.71	5.18	1.42	$6.11 \cdot 10^{-10}$
6'	C36-H6Y	-0.26	2.75	0.71	-	-	-
7'	C37-H7X	-0.26	2.24	0.65	5.00	1.30	$5.97 \cdot 10^{-10}$
7'	C37-H7Y	-0.26	2.76	0.65	-	-	-
8'	C38-H8X	-0.26	2.29	0.61	4.68	1.23	$5.61 \cdot 10^{-10}$
8'	C38-H8Y	-0.26	2.39	0.61	-	-	-
9'	C39-H9X	-0.24	2.05	0.58	4.22	1.16	$4.95 \cdot 10^{-10}$
9'	C39-H9Y	-0.24	2.18	0.58	-	-	-
R10	C10S-H10S	-0.29	3.37	0.78	7.71	1.56	$9.89 \cdot 10^{-10}$
R10	C10S-H10T	-0.29	4.34	0.78	-	-	-
R9	C9S-H9S	-0.28	3.47	0.86	7.59	1.73	$9.48 \cdot 10^{-10}$
R9	C9S-H9T	-0.28	4.12	0.86	-	-	-
R8'	C8F-H8F	-0.28	4.31	0.69	7.52	1.39	$9.69 \cdot 10^{-10}$
R8'	C8F-H8G	-0.28	3.20	0.70	-	-	-
R9'	C9F-H9F	-0.27	3.04	0.63	5.45	1.26	$6.73 \cdot 10^{-10}$
R9'	C9F-H9G	-0.27	2.41	0.63	-	-	-
R7	C7S-H7S	-0.27	9.30	1.27	19.04	2.55	$2.56 \cdot 10^{-9}$
R7	C7S-H7T	-0.27	9.75	1.27	-	-	-
R8	C8S-H8S	-0.29	5.81	1.13	13.39	2.25	$1.77 \cdot 10^{-9}$
R8	C8S-H8T	-0.29	7.58	1.12	-	-	-
R6'	C6F-H6F	-0.28	7.40	0.88	12.97	1.77	$1.74 \cdot 10^{-9}$
R6'	C6F-H6G	-0.27	5.56	0.89	-	-	-
R7'	C7F-H7F	-0.28	4.87	0.76	8.39	1.54	$1.08 \cdot 10^{-9}$
R7'	C7F-H7G	-0.28	3.51	0.77	-	-	-
R16	C16S-H16S	-0.20	0.95	0.31	2.07	0.63	$2.29 \cdot 10^{-10}$
R16	C16S-H16T	-0.20	1.11	0.31	-	-	-
R14'	C14F-H14F	-0.18	1.02	0.32	1.99	0.64	$2.13 \cdot 10^{-10}$
R14'	C14F-H14G	-0.18	0.97	0.32	-	-	-
14'	C314-H14X	-0.15	0.90	0.31	1.72	0.62	$1.78 \cdot 10^{-10}$
14'	C314-H14Y	-0.15	0.82	0.31	-	-	-
16	C216-H16R	-0.15	0.87	0.33	1.60	0.67	$1.56 \cdot 10^{-10}$
16	C216-H16S	-0.15	0.73	0.33	-	-	-
2'	C32-H2X	-0.26	8.62	1.07	19.13	2.15	$2.58 \cdot 10^{-9}$
2'	C32-H2Y	-0.24	10.50	1.08	-	-	-
2	C22-H2R	-0.08	23.23	1.59	41.21	3.18	$5.41 \cdot 10^{-9}$
2	C22-H2S	-0.13	17.97	1.59	-	-	-

R2'	C2F-H2F	-0.12	147.48	1.23	245.56	2.45	$3.41 \cdot 10^{-8}$
R2'	C2F-H2G	-0.10	98.07	1.21	-	-	-
III3	C3-H31	0.17	220.31	1.39	388.61	2.99	$5.59 \cdot 10^{-8}$
III3	C3-H32	-0.08	168.30	1.59	-	-	-
III5	C5-H5	0.10	211.32	1.49	211.32	1.49	$5.92 \cdot 10^{-8}$
R2	C2S-H2S	-0.38	125.34	0.66	125.34	0.66	$4.00 \cdot 10^{-8}$
γ	C13-H13A	0.01	1.57	1.36	4.72	4.08	$1.44 \cdot 10^{-10}$
γ	C13-H13B	0.01	1.56	1.36	-	-	-
γ	C13-H13C	0.01	1.60	1.36	-	-	-
γ	C14-H14A	0.01	1.64	1.36	4.95	4.08	$1.65 \cdot 10^{-10}$
γ	C14-H14B	0.01	1.66	1.36	-	-	-
γ	C14-H14C	0.02	1.65	1.36	-	-	-
γ	C15-H15A	0.01	1.62	1.36	4.81	4.08	$1.52 \cdot 10^{-10}$
γ	C15-H15B	0.01	1.56	1.36	-	-	-
γ	C15-H15C	0.01	1.63	1.36	-	-	-
α	C11-H11A	0.03	7.67	2.14	15.12	4.28	$1.68 \cdot 10^{-9}$
α	C11-H11B	0.02	7.45	2.14	-	-	-
I6	C6-H61	0.35	33.12	1.68	109.15	3.43	$1.80 \cdot 10^{-8}$
I6	C6-H62	0.06	76.03	1.75	-	-	-
II6	C6-H61	0.13	59.61	1.85	105.50	3.83	$1.36 \cdot 10^{-8}$
II6	C6-H62	-0.01	45.89	1.98	-	-	-
g1	C1-HX	-0.20	30.66	1.74	83.92	3.42	$1.08 \cdot 10^{-8}$
g1	C1-HY	-0.04	53.26	1.68	-	-	-
III9	C9-H91	-0.08	54.61	1.98	84.22	3.91	$1.23 \cdot 10^{-8}$
III9	C9-H92	-0.07	29.61	1.93	-	-	-
g3	C3-HA	-0.24	20.83	1.93	41.44	3.88	$5.67 \cdot 10^{-9}$
g3	C3-HB	-0.25	20.61	1.95	-	-	-
β	C12-H12A	-0.09	8.03	2.12	15.55	4.25	$1.75 \cdot 10^{-9}$
β	C12-H12B	-0.09	7.52	2.13	-	-	-
II4	C4-H4	0.17	319.71	1.01	319.71	1.01	$9.15 \cdot 10^{-8}$
III4	C4-H4	0.03	154.54	1.52	154.54	1.52	$4.23 \cdot 10^{-8}$
III7	C7-H7	-0.13	162.89	1.35	162.89	1.35	$4.56 \cdot 10^{-8}$
II2	C2-H2	-0.29	119.75	1.35	119.75	1.35	$3.59 \cdot 10^{-8}$
R1	C1S-H1S	-0.32	140.57	0.66	257.75	1.34	$4.12 \cdot 10^{-8}$
R1	C1S-H1T	-0.37	117.18	0.68	-	-	-
g2	C2-HS	-0.22	29.68	1.79	29.68	1.79	$8.22 \cdot 10^{-9}$
III8	C8-H8	0.15	88.16	1.80	88.16	1.80	$2.47 \cdot 10^{-8}$
III6	C6-H6	0.16	260.72	1.48	260.72	1.48	$7.42 \cdot 10^{-8}$
I2	C2-H2	-0.36	112.98	0.91	112.98	0.91	$3.54 \cdot 10^{-8}$
I3	C3-H3	-0.36	112.67	0.92	112.67	0.92	$3.52 \cdot 10^{-8}$
I5	C5-H5	-0.37	105.58	0.92	105.58	0.92	$3.34 \cdot 10^{-8}$
II5	C5-H5	-0.27	126.71	1.37	126.71	1.37	$3.75 \cdot 10^{-8}$
II3	C3-H3	-0.29	119.96	1.39	119.96	1.39	$3.58 \cdot 10^{-8}$
I4	C4-H4	-0.36	105.55	0.95	105.55	0.95	$3.31 \cdot 10^{-8}$
I1	C1-H1	-0.37	109.45	0.89	109.45	0.89	$3.47 \cdot 10^{-8}$
II1	C1-H1	-0.27	136.38	1.37	136.38	1.37	$4.02 \cdot 10^{-8}$
10	C210-H101	-0.06	2.08	1.39	2.08	1.39	$2.87 \cdot 10^{-10}$

9	C29-H91	-0.07	2.12	1.20	2.12	1.20	3.36·10⁻¹⁰
R4	C4S-H4S	-0.16	103.21	1.35	103.21	1.35	2.88·10⁻⁸
R5	C5S-H5S	-0.16	102.43	1.39	102.43	1.39	2.86·10⁻⁸

Table S4: NMR-derived order parameters $|S_{CH}|$, effective correlation times τ_e and $R_{1\rho}$ and R_1 relaxation rate constants for POPC at 303 K.

Carbon label	δ^{13}C (ppm)	δ^1H (ppm)	$|S_{CH}|$ (manual)	$|S_{CH}|$ (fit)	$R_{1\rho}$ (s⁻¹)	R_1 (s⁻¹)	τ_e (s)
18,16′	14	0.88	0.00	0.02	1.62	0.35	1.24·10⁻¹⁰
17,15'	22.82	1.29	0.06	0.07	2.65	0.63	2.99·10⁻¹⁰
3,3'	25.09	1.59	0.18	0.18	9.22	2.22	1.07·10⁻⁹
8	27.37	2.02	0.11	-	-	-	-
11	27.52	2.02	0.05	-	-	-	-
4	29.39	1.32	0.18	-	-	-	-
14,15	29.62	1.32	0.08	-	-	-	-
12'	29.76	1.32	0.10	-	-	-	-
4'	29.76	1.32	0.19	-	-	-	-
6	29.76	1.32	0.16	-	-	-	-
13,13'	29.91	1.32	0.09	-	-	-	-
5	29.91	1.32	0.18	-	-	-	-
5'	30.02	1.32	0.19	-	-	-	-
12	30.02	1.32	0.09	-	-	-	-
10'	30.13	1.32	0.14	-	-	-	-
11'	30.13	1.32	0.13	-	-	-	-
7	30.24	1.32	0.14	-	-	-	-
6'	30.37	1.32	0.18	0.19	15.78	1.32	2.10·10⁻⁹
7'	30.43	1.32	0.18	0.19	15.78	1.32	2.10·10⁻⁹
8'	30.46	1.32	0.16	0.19	15.78	1.32	2.10·10⁻⁹
9'	30.52	1.32	0.16	0.19	15.78	1.32	2.10·10⁻⁹
16,14′	32.19	1.26	0.08	0.09	3.54	0.82	4.03·10⁻¹⁰
2,2'	34.16	2.31	0.19	0.17	13.89	2.85	1.63·10⁻⁹
γ	54.23	3.23	0.00	0.01	2.41	2.09	7.44·10⁻¹¹
α	59.64	4.27	0.05	0.06	4.55	2.40	3.73·10⁻¹⁰
g1	63.18	4.22	0.14	0.22	15.67	4.28	1.07·10⁻⁹
g1	63.18	4.42	0.21	0.24	15.67	4.28	2.34·10⁻⁹
g3	63.82	3.99	0.14	0.15	18.97	4.68	2.13·10⁻⁹
g3	63.82	3.99	0.09	0.01	18.97	4.68	2.16·10⁻⁹
B	66.19	3.67	0.04	0.05	3.84	2.35	2.81·10⁻¹⁰
g2	70.78	5.26	0.20	0.20	10.07	3.15	2.19·10⁻⁹
10	129.49	5.3	0.03	0.02	2.41	1.87	2.70·10⁻¹⁰
9	129.84	5.32	0.09	0.11	3.67	1.65	6.68·10⁻¹⁰

Table S5: MD-derived order parameters S_{CH}, effective correlation times τ_e and $R_{1\rho}$ and R_1 relaxation rate constants calculated with Eq. S1, 4, 6 and 7 respectively for POPC at 303 K. The relaxation value for each carbon used to calculate τ_e is the sum of the contributions from all individual bonded protons.

Carbon label	C-H pair	S_{CH}	$R_{1\rho}$ (s^{-1})	R_1 (s^{-1})	Sum $R_{1\rho}$ (s^{-1})	Sum R_1 (s^{-1})	τ_e (s)
16'	C316-H16X	-0.03	0.11	0.10	0.33	0.29	$9.07 \cdot 10^{-12}$
16'	C316-H16Y	-0.03	0.11	0.10	-	-	-
16'	C316-H16Z	-0.03	0.11	0.10	-	-	-
18	C218-H18R	-0.03	0.10	0.10	0.31	0.29	$7.74 \cdot 10^{-12}$
18	C218-H18S	-0.03	0.10	0.10	-	-	-
18	C218-H18T	-0.03	0.11	0.10	-	-	-
15'	C315-H15X	-0.09	0.30	0.24	0.59	0.48	$3.14 \cdot 10^{-11}$
15'	C315-H15Y	-0.09	0.29	0.24	-	-	-
17	C217-H17R	-0.08	0.30	0.24	0.60	0.49	$3.13 \cdot 10^{-11}$
17	C217-H17S	-0.08	0.30	0.24	-	-	-
3'	C33-H3X	-0.18	2.20	0.98	4.53	1.96	$4.37 \cdot 10^{-10}$
3'	C33-H3Y	-0.16	2.34	0.98	-	-	-
3	C23-H3R	-0.20	3.38	1.31	5.98	2.69	$5.76 \cdot 10^{-10}$
3	C23-H3S	-0.21	2.61	1.38	-	-	-
8	C28-H8R	-0.10	1.48	1.02	2.96	2.03	$1.99 \cdot 10^{-10}$
8	C28-H8S	-0.10	1.48	1.01	-	-	-
11	C211-H11R	-0.08	1.05	0.85	2.12	1.70	$1.18 \cdot 10^{-10}$
11	C211-H11S	-0.08	1.07	0.85	-	-	-
4	C24-H4R	-0.20	2.25	1.01	4.32	2.05	$3.98 \cdot 10^{-10}$
4	C24-H4S	-0.20	2.07	1.04	-	-	-
14	C214-H14R	-0.13	0.79	0.56	1.58	1.12	$1.07 \cdot 10^{-10}$
14	C214-H14S	-0.13	0.80	0.56	-	-	-
15	C215-H15R	-0.12	0.63	0.46	1.24	0.93	$7.68 \cdot 10^{-11}$
15	C215-H15S	-0.12	0.62	0.46	-	-	-
12'	C312-H12X	-0.15	0.77	0.52	1.52	1.04	$1.06 \cdot 10^{-10}$
12'	C312-H12Y	-0.16	0.75	0.52	-	-	-
4'	C34-H4X	-0.21	1.76	0.84	3.65	1.68	$3.45 \cdot 10^{-10}$
4'	C34-H4Y	-0.20	1.89	0.84	-	-	-
6	C26-H6R	-0.19	1.80	0.88	3.57	1.75	$3.22 \cdot 10^{-10}$
6	C26-H6S	-0.19	1.77	0.88	-	-	-
13'	C313-H13X	-0.13	0.62	0.45	1.22	0.89	$7.76 \cdot 10^{-11}$
13'	C313-H13Y	-0.13	0.60	0.45	-	-	-
13	C213-H13R	-0.13	0.86	0.63	1.73	1.26	$1.11 \cdot 10^{-10}$
13	C213-H13S	-0.13	0.87	0.63	-	-	-
5	C25-H5R	-0.21	2.15	0.90	4.14	1.82	$4.01 \cdot 10^{-10}$
5	C25-H5S	-0.21	1.99	0.92	-	-	-
5'	C35-H5X	-0.21	1.66	0.75	3.42	1.51	$3.31 \cdot 10^{-10}$
5'	C35-H5Y	-0.20	1.76	0.75	-	-	-
12	C212-H12R	-0.12	1.00	0.72	1.99	1.44	$1.28 \cdot 10^{-10}$
12	C212-H12S	-0.12	1.00	0.72	-	-	-
10'	C310-H10X	-0.18	1.10	0.61	2.14	1.22	$1.78 \cdot 10^{-10}$
10'	C310-H10Y	-0.18	1.04	0.61	-	-	-
11'	C311-H11X	-0.17	0.88	0.58	1.76	1.15	$1.30 \cdot 10^{-10}$

11'	C311-H11Y	-0.17	0.88	0.58	-	-	-
7	C27-H7R	-0.18	1.68	0.86	3.31	1.73	$2.86 \cdot 10^{-10}$
7	C27-H7S	-0.18	1.63	0.87	-	-	-
6'	C36-H6X	-0.22	1.53	0.72	3.15	1.44	$3.01 \cdot 10^{-10}$
6'	C36-H6Y	-0.22	1.62	0.72	-	-	-
7'	C37-H7X	-0.21	1.40	0.68	2.79	1.36	$2.58 \cdot 10^{-10}$
7'	C37-H7Y	-0.21	1.40	0.68	-	-	-
8'	C38-H8X	-0.21	1.28	0.66	2.56	1.32	$2.30 \cdot 10^{-10}$
8'	C38-H8Y	-0.21	1.28	0.66	-	-	-
9'	C39-H9X	-0.19	1.17	0.64	2.33	1.28	$2.00 \cdot 10^{-10}$
9'	C39-H9Y	-0.19	1.16	0.64	-	-	-
14'	C314-H14X	-0.12	0.45	0.34	0.90	0.69	$5.29 \cdot 10^{-11}$
14'	C314-H14Y	-0.12	0.45	0.34	-	-	-
16	C216-H16R	-0.11	0.48	0.36	0.97	0.72	$5.97 \cdot 10^{-11}$
16	C216-H16S	-0.11	0.49	0.36	-	-	-
2'	C32-H2X	-0.24	3.10	1.11	6.80	2.23	$7.50 \cdot 10^{-10}$
2'	C32-H2Y	-0.21	3.71	1.12	-	-	-
2	C22-H2R	-0.07	7.08	1.62	12.98	3.30	$1.53 \cdot 10^{-9}$
2	C22-H2S	-0.11	5.90	1.68	-	-	-
γ	C13-H13A	0.01	1.04	0.98	3.10	2.94	$7.18 \cdot 10^{-11}$
γ	C13-H13B	0.01	1.03	0.98	-	-	-
γ	C13-H13C	0.01	1.03	0.98	-	-	-
γ	C14-H14A	0.01	1.03	0.98	3.09	2.94	$7.08 \cdot 10^{-11}$
γ	C14-H14B	0.01	1.02	0.98	-	-	-
γ	C14-H14C	0.01	1.03	0.98	-	-	-
γ	C15-H15A	0.01	1.03	0.98	3.08	2.94	$7.03 \cdot 10^{-11}$
γ	C15-H15B	0.01	1.03	0.98	-	-	-
γ	C15-H15C	0.01	1.03	0.98	-	-	-
α	C11-H11A	0.03	2.40	1.78	4.82	3.57	$3.09 \cdot 10^{-10}$
α	C11-H11B	0.03	2.42	1.79	-	-	-
g1	C1-HX	-0.18	8.42	2.43	23.51	4.76	$2.58 \cdot 10^{-9}$
g1	C1-HY	-0.04	15.09	2.33	-	-	-
g3	C3-HA	-0.23	7.62	2.15	14.39	4.37	$1.64 \cdot 10^{-9}$
g3	C3-HB	-0.25	6.78	2.21	-	-	-
β	C12-H12A	-0.08	2.33	1.75	4.64	3.50	$2.91 \cdot 10^{-10}$
β	C12-H12B	-0.08	2.31	1.75	-	-	-
g2	C2-HS	-0.20	8.33	2.56	8.33	2.56	$1.91 \cdot 10^{-9}$
10	C210-H101	-0.05	1.63	1.34	1.63	1.34	$1.69 \cdot 10^{-10}$
9	C29-H91	-0.06	1.64	1.18	1.64	1.18	$2.04 \cdot 10^{-10}$

References

1. M. J. Abraham, T. Murtola, R. Schulz, S. Páll, J. C. Smith, B. Hess and E. Lindahl, *SoftwareX*, 2015, **1**, 19-25.
2. J. B. Klauda, R. M. Venable, J. A. Freites, J. W. O'Connor, D. J. Tobias, C. Mondragon-Ramirez, I. Vorobyov, A. D. MacKerell Jr and R. W. Pastor, *J. Phys. Chem. B*, 2010, **114**, 7830-7843.
3. W. Jorgensen, J. Chandrasekhar, J. Madura, R. Impey and M. Klein, *J. Chem. Phys.*, 1983, **79**, 926-935.
4. A. D. MacKerell Jr, D. Bashford, M. Bellott, R. L. Dunbrack Jr, J. D. Evanseck, M. J. Field, S. Fischer, J. Gao, H. Guo and S. Ha, *J. Phys. Chem. B*, 1998, **102**, 3586-3616.
5. J. Lee, D. S. Patel, J. Ståhle, S.-J. Park, N. R. Kern, S. Kim, J. Lee, X. Cheng, M. A. Valvano and O. Holst, *J. Chem. Theory Comput.*, 2018, **15**, 775-786.
   T. Darden, G. York and L. Pedersen, *J. Chem. Phys.*, 1993, **98**, 10089.
6. B. Hess, H. Bekker, H. J. C. Berendsen and J. G. E. M. Fraaije, *J. Comput. Chem.*, 1997, **18**, 1463-1472.
7. S. Miyamoto and P. A. Kollman, *J. Comput. Chem*, 1992, **13**, 952-962.
8. S. Nose, *Mol. Phys.*, 1984, **52**, 255-268.
9. W. G. Hoover, *Phys. Rev. A*, 1985, **31**, 1695-1697.
10. M. Parrinello and A. Rahman, *J. Appl. Phys.*, 1981, **52**, 7182-7190.
11. A. Botan, F. Favela-Rosales, P. F. J. Fuchs, M. Javanainen, M. Kanduč, W. Kulig, A. Lamberg, C. Loison, A. Lyubartsev, M. S. Miettinen, L. Monticelli, J. Määttä, O. H. S. Ollila, M. Retegan, T. Róg, H. Santuz and J. Tynkkynen, *J. Chem. Phys. B*, 2015, **119**, 15075-15088.
12. The NMRlipids project, http://nmrlipids.blogspot.com, (accessed May, 2022).
13. N. Kucerka, J. F. Nagle, J. N. Sache, S. E. Feller, J. Pencer, A. Jackson and J. Katsaras, *Biophys. J.*, 2008, N. Kucerka, **95**, 2356-2367.
14. X. Zhuang, J. R. Makover, W. Im and J. B. Klauda, *BBA*, 2014, **1838**, 2520-2529.
15. H. I Petrache, S. E. Feller and J. F. Nagle, *Biophys. J.*, 1997, **70**, 2237-2242.
16. N. Kucerka, M-P Nieh, and J. Katsaras, *BBA*, 2011, **1808**, 2761-2771.
17. A. Bax, D. G. Davis and S. K. Sarkar, *J. Magn. Reson.*, 1985, **63**, 230-234.
18. S. V. Dvinskikh, V. Castro and D. Sandström, *Phys. Chem. Chem. Phys.*, 2005, **7**, 607-613.
19. T. M. Ferreira, F. Coreta-Gomes, O. S. Olila, M. J. Moreno, W. L. Vaz and D. Topgaard, *Phys. Chem. Chem. Phys.*, 2013, **15**, 1976-1989.
20. T. M. Ferreira, B. Medronho, R. W. Martin and D. Topgaard, *Phys. Chem. Chem. Phys.*, 2008, **10**, 6033-6038.